AIP | Applied Physics Letters

Subpicosecond electron-hole recombination time and terahertz-bandwidth photoresponse in freestanding GaAs epitaxial mesoscopic structures

Martin Mikulics, Jie Zhang, John Serafini, Roman Adam, Detlev Grützmacher et al.

Citation: Appl. Phys. Lett. **101**, 031111 (2012); doi: 10.1063/1.4737442
View online: http://dx.doi.org/10.1063/1.4737442
View Table of Contents: http://apl.aip.org/resource/1/APPLAB/v101/i3
Published by the American Institute of Physics.

Subpicosecond electron-hole recombination time and terahertz-bandwidth photoresponse in freestanding GaAs epitaxial mesoscopic structures

Martin Mikulics,[1] Jie Zhang,[2] John Serafini,[3] Roman Adam,[4] Detlev Grützmacher,[1] and Roman Sobolewski[2,3,a)]

[1]*Peter Grünberg Institut PGI-9, Forschungszentrum Jülich, D-52425 Jülich, Germany and Jülich-Aachen Research Alliance (JARA)—Fundamentals of Future Information Technology, D-52425 Jülich, Germany*
[2]*Department of Electrical and Computer Engineering and Laboratory for Laser Energetics, University of Rochester, Rochester, New York 14627-0231, USA*
[3]*Department of Physics and Astronomy and Laboratory for Laser Energetics, University of Rochester, Rochester, New York 14627-0231, USA*
[4]*Peter Grünberg Institut PGI-6, Forschungszentrum Jülich, D-52425 Jülich, Germany*

(Received 18 May 2012; accepted 2 July 2012; published online 18 July 2012)

We present the ultrafast (THz-bandwidth) photoresponse from GaAs single-crystal mesoscopic structures, such as freestanding whiskers and platelets fabricated by the top-down technique, transferred onto a substrate of choice, and incorporated into a coplanar strip line. We recorded electrical transients as short as ~600 fs from an individual whisker photodetector. Analysis of the frequency spectrum of the photoresponse electrical signal showed that, intrinsically, our device was characterized by an ~150-fs carrier lifetime and an overall 320-fs response. The corresponding 3-dB frequency bandwidth was 1.3 THz—the highest bandwidth ever reported for a GaAs-based photodetector. Simultaneously, as high-quality, epitaxially grown crystals, our GaAs structures exhibited mobility values as high as ~7300 $cm^2/V \cdot s$, extremely low dark currents, and ~7% intrinsic detection efficiency, which, together with their experimentally measured photoresponse repetition time of ~1 ps, makes them uniquely suitable for terahertz-frequency optoelectronic applications, ranging from ultrafast photon detectors and counters to THz-bandwidth optical-to-electrical transducers and photomixers. © *2012 American Institute of Physics*.
[http://dx.doi.org/10.1063/1.4737442]

Ultrahigh-speed photonic devices, such as ultrafast photoswitches, photomixers, and photodetectors, based on III–V semiconducting compounds, have been studied intensively in recent years,[1,2] with special emphasis focused on the GaAs material because of its excellent electronic transport and optoelectronic properties. GaAs-based devices are commonly used in high-end commercial applications, such as satellite communication systems and radar.[3] The so-called low-temperature-grown GaAs (LT-GaAs) material plays a special role, since it exhibits a <200-fs carrier lifetime and, as a result, has been widely implemented in the fastest photodetectors[4,5] and THz photomixers.[6] Independently, during the last decade, there has been an explosive growth of a new generation of devices based on low-dimensional, nanometer-sized structures. Among them, the most popular are single-crystal semiconducting nanowhiskers and nanowires, which have demonstrated a unique potential in photonics applications.[7–10]

Here we report on our measurements of a femtosecond photoresponse from freestanding, submicrometer-sized GaAs whiskers and platelets fabricated from an epitaxial GaAs layer in a top-down etching process and incorporated into a coplanar-strip (CPS) transmission line. Our fabrication process started with the molecular beam epitaxy (MBE) growth of a planar GaAs back layer on a semi-insulating GaAs substrate, followed by a 50-nm-thick AlAs sacrificial interlayer, and, finally, a 500-nm-thick top GaAs layer. The growth process was performed at 600 °C in order to obtain GaAs of the highest quality. After the MBE growth, an array of 500-nm-wide whisker structures was patterned by employing optical lithography and argon-ion–beam etching. Next, our patterned whiskers were detached from their native substrate by dissolving the AlAs layer in a HF:H_2O solution and, subsequently, placed on a single-crystal MgO substrate with the help of a special micropipette. The entire procedure of whisker fabrication, transfer, and positioning is shown schematically in Fig. 1. Compared to our earlier-described fabrication processes,[11,12] we employed a micrometer-sized, quartz-glass pipette for precise manipulation and transfer of

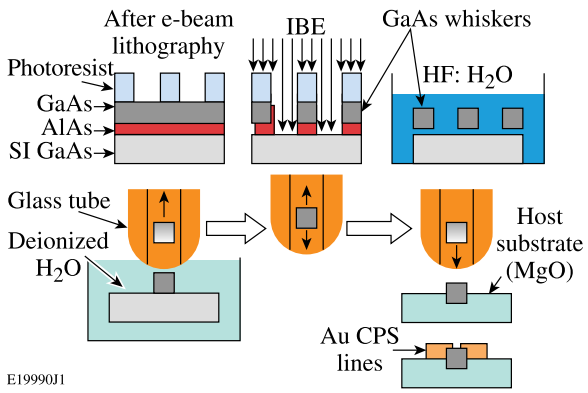

FIG. 1. Top-down fabrication and transfer process of a freestanding, single-crystal GaAs mesoscopic structure integrated in a CPS transmission line.

a)Author to whom correspondence should be addressed. Electronic mail: roman.sobolewski@rochester.edu. Also at the Institute of Electron Technology, PL-02668 Warszawa, Poland.

our whisker to a designated, pre-etched trench position on a host MgO substrate. Using a pipette, we achieved an overall, 5- to 10-μm accuracy of the whisker positioning. The bond of our mesoscopic GaAs rods to the MgO substrate was strong enough to allow for the subsequent, standard photolithography processing and deposition of 20-μm-wide, 10-μm-separation Au CPS transmission lines on top of the ends of the whisker (see the bottom inset in Fig. 2). To improve morphology and crystallinity of the GaAs whiskers and to eliminate possible defects on their sidewalls, the entire structure was annealed for 20 min for 600 °C in a nitrogen atmosphere, following Krotkus *et al.*[13] During the annealing, the whisker structures were covered with a dummy GaAs substrate to suppress arsenic reduction.

Electrical characterization of our CPS-imbedded whisker photodetector structures (10 μm long with a 500×500-nm^2 cross-section) was carried out by measuring the current–voltage (I–V) characteristics both in the dark and under 850-nm-wavelength continuous-wave light illumination with the nominal power of 0.2 mW. Note that the I–V curves shown in Fig. 2 exhibit an ohmic behavior in the tested bias range. The sample resistivity was calculated to be 5×10^4 Ω cm, so our device is an *n*-type, semi-insulated GaAs crystal with $n_0 \approx 2 \times 10^{10}$ cm^{-3}. Space-charge effects were not observed, which indicated an efficient suppression of the high-field region near the contacts. The dark current values were 5.2×10^{-10} A at 10 V and about 2×10^{-9} A at 30 V and were approximately an order of magnitude lower than the ones measured earlier in freestanding LT-GaAs photodetectors.[4,12] The top inset in Fig. 2 shows the responsivity of our device as a function of the bias voltage. The responsivity was calculated for the actual light power of ~0.12 mW delivered to the whisker and normalized to its photoactive area of 0.5×10 μm^2 (see inset in Fig. 2) and reached 4.4 mA/W at the 30-V bias, which corresponded to ~7% photon-detection efficiency.

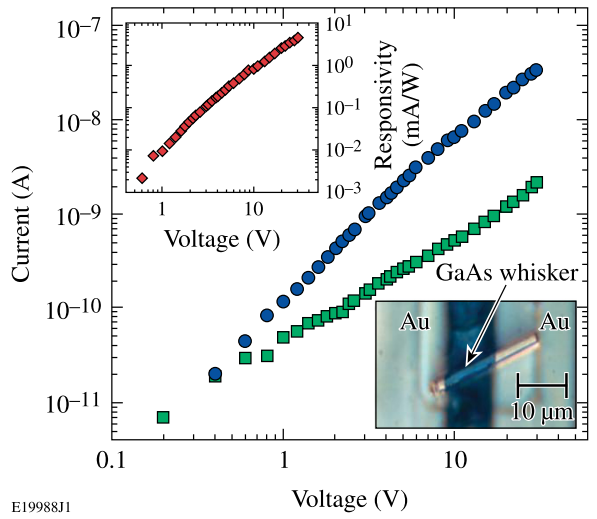

FIG. 2. Current–voltage characteristics of a GaAs freestanding whisker placed on an MgO substrate and incorporated in a CPS transmission line (see bottom inset). The characteristics were measured in the dark (green squares) and under 850-nm-wavelength, 0.2-mW nominal incident power, continuous illumination (dark blue dots), respectively. The top left inset presents the responsivity of our device as a function of bias. The bottom right inset shows a top-view micrograph of the whisker incorporated into the Au CPS line. The blue part is the bare MgO substrate.

Time-resolved measurements of the whisker photoresponse were performed using our time-resolved, electro-optic (EO) sampling system reported earlier in Ref. 4. Briefly, the photoresponse electrical transients were measured using a $LiTaO_3$ crystal with a bottom high-reflectivity coating as the ultrafast EO transducer. Electrical transients were generated by uniformly exciting (beam diameter ~30 μm) the whisker with 100-fs-duration, 800-nm-wavelength laser pulses. Next, they were coupled via the 45-Ω characteristic impedance CPS into the EO crystal and—by means of the Pockels effect—converted into the change of the polarization state of optical sampling pulses incident on $LiTaO_3$ and time correlated with the excitation pulses. Figure 3(a) shows two experimental electrical response waveforms (black lines) collected by positioning the sampling beam near the EO sensor edge at points 137 μm and 171 μm away from the whisker, respectively [see Fig. 3(a) inset]. The experimental transients were fitted (smooth red lines) using an error function (pulse rise) followed by an exponential decay in order to properly represent both the rising and falling edges of the measured pulses. We note an excellent overlap of the experimental data and fits. The waveform recorded at the 137-μm point exhibits a full width at half maximum (FWHM) equal to 660 fs and a 490-fs fall time, while the pulse at 171 μm has a FWHM equal to 720 fs and a decay time of 550 fs. The observed slight change in the shape of the latter pulse (e.g., lower amplitude) is due to signal distortion (attenuation and dispersion) during propagation along the CPS line.

We have collected several photoresponse transients along the CPS line, starting with the distance ~100 μm away of the whisker, and their values of FWHM (triangles) are plotted in Fig. 3(b). Next, we performed a standard frequency-domain analysis[14] of our signals in order to first determine the amount of distortion introduced by our CPS line and, subsequently, to calculate the actual intrinsic transient generated by the photodetector, by "back-propagating" an experimental transient, e.g., the one measured at 137 μm, toward its zero-distance plane (whisker position) on the CPS line.

It is well known that in passive transmission lines, by using the Fourier transform approach, one can retrieve the temporal shape of a voltage pulse $V(z, t)$ at the position z from the known $V(z_1, t)$ transient measured at a different point z_1 along the line, if one knows the spectral characteristics of the complex propagation factor $\gamma(f)$ of the transmission line.[14] The $\gamma(f)$ factor can, in turn, be computed numerically by comparing frequency spectra (taking their ratio) of two (or more for better accuracy) experimental waveforms, measured at different positions along the transmission line. Using the above approach, we have extracted the $\gamma(f)$ spectral dependence for our CPS line based on the experimental transients recorded at the positions along the CPS line indicated in Fig. 3(b). Next, using our $\gamma(f)$ factor and the Fourier transform of the signal collected at the 137-μm point [see Fig. 3(a)], we reproduced the temporal shape of the signal generated at the whisker plane [$V(z = 0, t)$]. The resulting intrinsic signal generated by our photodetector had a peak amplitude $V_s = 185.7$ mV, FWHM = 320 fs, and a fall time of ~150 fs. The rising edge was limited by the 100-fs width of our optical excitation pulse. The 320-fs response time of our device is at least one order of magnitude faster than any

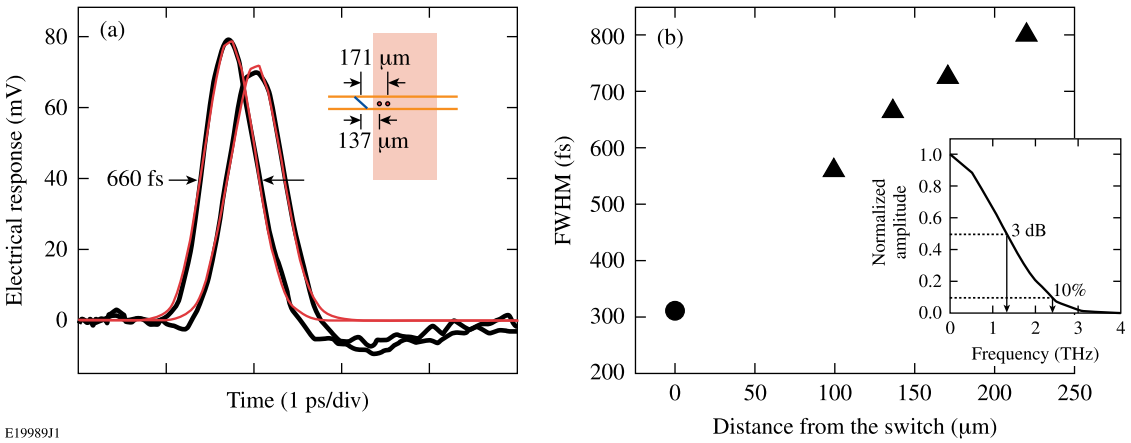

FIG. 3. (a) Transient photoresponses of a GaAs whisker photodetector illuminated with a 100-fs-wide, 800-nm-wavelength, and 1-mW incident power optical pulse. The detector bias was 20 V. The black curves are experimental data recorded at 137-μm and 171-μm positions away from the device (see inset), respectively, while smooth, red curves are numerical fits. The time interval between the two pulses is 294 fs and directly corresponds to the 34 μm of the propagation distance along the CPS. We note that in order to avoid excessive pulse distortion the sampling beam was always placed at the edge of the $LiTaO_3$ crystal, i.e., the EO sensor was slightly moved when we switched from the 137-μm point to the 171-μm point. (b) FWHM values of experimental transients (solid triangles) recorded at several distances along the CPS away from the detector plane. The solid dot represents the 320-fs FWHM value of the intrinsic pulse generated by the whisker. The inset in (b) shows the spectral characteristics of the calculated, intrinsic, zero-propagation distance transient. The 3-dB and 10% spectral ranges are marked.

demonstrated nanostructures.[15] The FWHM value of $V(0, t)$ is indicated in Fig. 3(b) by a solid dot, while the inset in Fig. 3(b) presents its spectral characteristics. We note that our intrinsic photoresponse signal has a 3-dB bandwidth up to 1.3 THz and a 10% bandwidth of above 2.4 THz, making the GaAs single-crystal whisker a truly THz-signal generator.

For our CPS line, we also calculated the phase factor $\beta(f) = \mathrm{Im}[\gamma(f)]$, which was a linear function of f and allowed us to directly determine the signal propagation phase velocity as equal to 1.16×10^8 m/s. The latter value agrees very well with the one computed using the propagation parameters of the two pulses presented in Fig. 3(a).

In addition to whiskers, we have studied the 500-nm-thick, 10×10-μm^2-active-area, platelet-type photodetectors to determine if the performance of our whisker was geometry limited or if it resulted from the intrinsic properties of the 500-nm-thick epitaxial GaAs film. In both the whisker and platelet cases, we measured the dependence of the photoresponse pulse FWHM and V_s on the applied dc bias and incident optical power. The results were qualitatively identical in the tested 0- to 30-V bias range (equipment limited). Under the fixed (low) optical excitation power, the photoresponse FWHM remained constant, while V_s increased linearly with the bias. The FWHM also remained constant over the tested range of the incident optical power, while V_s initially increased linearly and started to saturate when the incident power exceeded 3 mW. The most striking observation, however, was that the photoresponse transients of platelet devices, measured under the same conditions as whiskers (e.g., the same sampling spot distance), exhibited practically the same ~670-fs values of the FWHM, clearly indicating that in both types of devices we observed the same ultrafast surface and bulk electron-hole recombination process, governed by the shortest device dimension, namely, its 500-nm thickness.

The transient photoresponse studies also allowed us to determine carrier mobility in our GaAs structures. Following Ref. 16, we used the expression for the total charge (integrated photocurrent) generated in our photodetector upon laser pulse excitation and, subsequently, compared it directly to the photoresponse signal (peak current $= V_s/45\ \Omega$). For calculations [see, e.g., Eq. (1) in Ref. 4], we used our experimental parameters for the optical excitation and sample geometry, as well as the responsivity value taken from the inset in Fig. 2 at the actual 20-V bias. Therefore, the only unknown parameter was the sample mobility, which turned out to be ~7300 cm^2/V s. We note that this is a very respectable (bulk-like) value for our mesoscopic structures and clearly indicates that, indeed, our devices are very high quality bars of the GaAs single crystal. The latter indicates that, contrary to conventional LT-GaAs photodetectors, trapping of photocarriers, although likely to occur at some surface states, cannot be the dominant mechanism responsible for the subpicosecond relaxation dynamics observed in our experiments. We stipulate that the main relaxation channel is the Shockley–Read–Hall-type recombination process under the very high level injection condition since, in our case, the concentration of photoexcited electrons is at least 10^5 times larger than n_0 and there is no out-diffusion of carriers due to the freestanding nature (GaAs on MgO) of our 500-nm-thick devices.

The latter conclusion was directly confirmed in another series of EO experiments, where in every laser cycle we excited our devices using a pair of 100-fs optical pulses with their separation externally controlled and varied from ~1 to 4 ps. In our results shown in Fig. 4, the main panel presents the double-pulse photoresponse when the excitation pluses were separated by 2.1 ps; one can clearly see that the magnitude of the photoresponse reaches zero between the two ~670-fs-wide pulses, meaning that our carriers excited by the first optical pulse managed to reach their equilibrium state before the arrival of the second pulse. The inset shows the case when the separation between the excitation pulses was only 1.1 ps, and even in this case, the carrier relaxation after the first excitation is over 90% complete. The latter experiment most directly confirms that the carrier recombination, and not the trapping, is responsible for the ultrafast

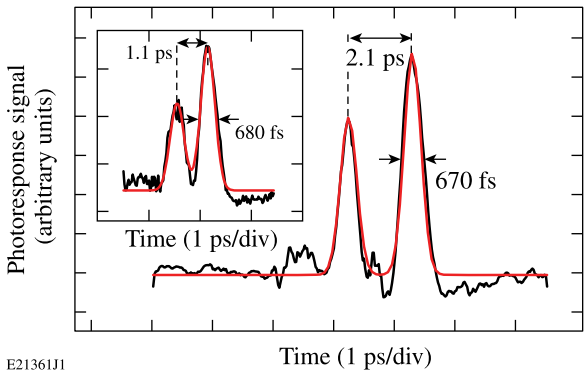

FIG. 4. Transient photoresponse of a GaAs platelet photodetector illuminated with a train of two 100-fs-wide, 800-nm-wavelength, and 1-mW incident power optical pulses. The detector bias was 20 V. The black line is an experimental signal recorded at ~150 μm away from the device plane [see inset in Fig. 3(a)], while the smooth, red line is a numerical fit representing a combination of the error functions (rise portions of the pulses) and the single-exponential decay (relaxation parts). The inset shows the experimental transients recorded when the separation between the laser pulses exciting the photodetector was 1.1 ps. The difference in the amplitudes of the first and second photoresponse pulses is due to an approximately 40/60 beam splitter used to generate a two-pulse excitation train.

photoresponse of our devices; it also demonstrates that our meso-structured detectors can very effectively operate even when they are exposed to optical input trains (e.g., optical clock signals) with a THz repetition rate.

In conclusion, the presented top-down technology of epitaxial growth and transfer of meso-structured, single-crystal GaAs devices provides a uniquely simple and reliable method to integrate photoconductive elements with ultrafast electronic and optoelectronic on-chip systems, ensuring an extremely wide (THz) bandwidth, high operating bias voltage, and high optical-power-handling capabilities. It should be noted that with our fabrication approach, the freestanding structures can be placed at virtually any point on a test circuit (in combination with various substrates), making them a very promising option for hybrid circuitry applications, where integration of various materials and test devices is required. They are also relatively easy to assemble into arrays for multichannel on-chip communication and detection. As a photodetector, the freestanding, epitaxial GaAs element is truly unique since it combines extremely low dark currents and ~7% single-photon detection efficiency with a subpicosecond photoresponse and ensures reliable and efficient operation even in optical systems with THz laser clock-pulse rates.

The authors thank P. Song and M. Samuels for their assistance in some experiments. This work was supported in part by NSF Grant No. ECCS-0901701 (Rochester). J.Z. and J.S. acknowledge support from the Frank Horton Graduate Fellowship Program at the University of Rochester's Laboratory for Laser Energetics, funded by the U.S. Department of Energy Office of Inertial Confinement Fusion under Cooperative Agreement No. DE-FC52-08NA28302 and the New York State Energy Research and Development Authority. The support of NSF and DOE does not constitute their endorsement of the views expressed in this article.

[1]*High-Speed Photonic Devices, Series in Optics and Optoelectronics*, edited by N. Dagli (Taylor & Francis, Boca Raton, FL, 2006), and references therein.
[2]G. Steinmeyer, J. Opt. A: Pure Appl. Opt. **5**, R1 (2003), and references therein.
[3]M. E. Kim, A. K. Oki, G. M. Gorman, D. K. Umemoto, and J. B. Camou, IEEE Trans. Microwave Theory Tech. **37**, 1286 (1989).
[4]X. Zheng, Y. Xu, R. Sobolewski, R. Adam, M. Mikulics, M. Siegel, and P. Kordoš, Appl. Opt. **42**, 1726 (2003).
[5]M. Mikulics, S. Wu, M. Marso, R. Adam, A. Förster, A. van der Hart, P. Kordoš, H. Lüth, and R. Sobolewski, IEEE Photonics Technol. Lett. **18**, 820 (2006).
[6]M. Mikulics, E. A. Michael, R. Schieder, J. Stutzki, R. Güsten, M. Marso, A. van der Hart, H. P. Bochem, H. Lüth, and P. Kordoš, Appl. Phys. Lett. **88**, 041118 (2006).
[7]K. Hiruma, M. Yazawa, T. Katsuyama, K. Ogawa, K. Haraguchi, M. Koguchi, and H. Kakibayashi, J. Appl. Phys. **77**, 447 (1995).
[8]Y. Cui, Q. Wei, H. Park, and C. M. Lieber, Science **293**, 1289 (2001).
[9]X. Duan, Y. Huang, Y. Cui, J. Wang, and C. M. Lieber, Nature **409**, 66 (2001).
[10]Y. Huang, X. Duan, Y. Cui, and C. M. Lieber, Nano Lett. **2**, 101 (2002).
[11]M. Mikulics, R. Adam, M. Marso, A. Förster, P. Kordoš, H. Lüth, S. Wu, X. Zheng, and R. Sobolewski, IEEE Photonics Technol. Lett. **17**, 1725 (2005).
[12]M. Marso, M. Mikulics, R. Adam, S. Wu, X. Zheng, I. Camara, F. Siebe, A. Forster, R. Gusten, P. Kordoš, and R. Sobolewski, Acta Phys. Pol. A **107**, 109 (2005).
[13]A. Kortkus, S. Marcinkevicius, J. Jasinski, M. Kaminska, H. H. Tan, and C. Jagadish, Appl. Phys. Lett. **66**, 3304 (1995).
[14]J. F. Whitaker, R. Sobolewski, D. R. Dykaar, T. Y. Hsiang, and G. A. Mourou, IEEE Trans. Microwave Theory Tech. **36**, 277 (1988).
[15]P. Parkinson, H. J. Joyce, Q. Gao, H. H. Tan, X. Zhang, J. Zou, C. Jagadish, L. M. Herz, and M. B. Johnston, Nano Lett. **9**, 3349 (2009).
[16]S. Gupta, J. F. Whitaker, and G. A. Mourou, IEEE J. Quantum Electron. **28**, 2464 (1992).